Russian Physics Journal, Vol. 56, No. 12, April, 2014 (Russian Original No. 12, December, 2013)

PHYSICS OF SEMICONDUCTORS AND DIELECTRICS

CHARACTERISTICS OF THE SEMICONDUCTOR RESISTIVE HYDROGEN SENSORS IN THE THERMO-CYCLIC OPERATION MODE

V. I. Gaman,[1] E. Yu. Sevast'yanov,[2] N. K. Maksimova,[2] A. V. Almaev,[1] N. S. Sergeichenko[2]

UDC 621.382

The results of studies of the time dependence of conductivity of hydrogen sensors, based on thin polycrystalline films of tin dioxide, in the thermo-cyclic operation mode, are presented. A method for determining the energy band bending at the interface of the contacting SnO_2 *microcrystals in the tin-dioxide film and two methods for measuring the low concentrations of hydrogen (*$n_{H_2} < 10^4$ *ppm) are proposed. It is shown that the sensors of this type in the thermo-cyclic operation mode are characterized by high values of the response to the impact of* H_2*, high sensitivity, and high speed.*

Keywords: gas sensor, tin dioxide, hydrogen, thermo-cyclic operation mode, energy band bending.

INTRODUCTION

In connection with the development of hydrogen energetic, an important task is to develop highly sensitive and high-speed sensors of molecular hydrogen. To solve this problem for the low concentrations $n_{H_2} \le 10^4$ ppm in the air, the semiconductor resistive sensors based on thin films of tin dioxide can be used [1, 2].

In the sensors of this type exposed to hydrogen, the over-barrier component of conductivity plays a decisive role. In the stationary regime, the response can be described by the following expression [1, 2]:

$$\frac{G_H(T)}{G_0(T)} = \exp\left[\frac{e\varphi_S(T)\eta_H n_{H_2}}{kT(1+\eta_H n_{H_2})}\left(2 - \frac{\eta_H n_{H_2}}{1+\eta_H n_{H_2}}\right)\right], \quad (1)$$

where G_H and G_0 are the conductivities of the sensor in the air + hydrogen mixture and clean air, respectively, $e\varphi_S$ is the energy band bending in the surface region of the SnO_2 microcrystals, e is the electron charge, φ_S is the surface potential, η_H is the coefficient proportional to the ratio of the probability of adsorption of a hydrogen atom on the surface of the semiconductor to the probability of its desorption, k is the Boltzmann constant, and T is the sensor absolute temperature.

The process of hydrogen adsorption on the film of tin dioxide is characterized by the value of η_H, which does not depend on the sensor temperature, n_{H_2}, and the humidity level of the gas mixture. The energy band bending $e\varphi_S$ depends on the oxygen concentration and humidity in the gas mixture.

To determine the concentration of hydrogen in the gas mixture, a calibration graph showing the dependence G_H/G_0 on n_{H_2} for a given sensor, can be used. However, since the humidity and oxygen concentration in the gas mixture

[1]National Research Tomsk State University, Tomsk, Russia, e-mail: gaman@elefot.tsu.ru; [2]V. D. Kuznetsov Siberian Physical-Technical Institute at National Research Tomsk State University, Tomsk, Russia. Translated from Izvestiya Vysshikh Uchebnykh Zavedenii, Fizika, No. 12, pp. 96–102, December, 2013. Original article submitted July 10, 2013.

can vary in time, it is problematic to use this method in practice. Moreover, the sensor characteristics can vary during storage and operation.

It follows from Eq. (1) that for a correct determination of n_{H_2}, the values of G_H, G_0, and $e\varphi_S$ should be measured simultaneously or with a small difference in time. It is shown that these measurements can be performed during operation of the sensor in the thermo-cyclic mode. Methods for determining n_{H_2} without using the calibration graph are proposed.

1. TIME DEPENDENCE OF THE SENSOR CONDUCTIVITY IN THE THERMO-CYCLIC MODE IN THE ATMOSPHERE OF CLEAN AIR

The sensor conductivity in the clean air is $G_0 = G_{0b} + G_{0ch}$, where G_{0b} and G_{0ch} are the over-barrier and channel components, respectively [2, 3]. The ratio between the values of G_{0b} and G_{0ch} depends on the microstructure of the tin-dioxide films and oxygen concentration in the air. Further, we consider sensors, for which $G_{0b} >> G_{0ch}$ and $G_0 \approx G_{0b}$. The realization of these experimental conditions is indicated by the presence of the superlinear dependence of the response on the hydrogen concentration in the case of low n_{H_2} ($\eta\, n_{H_2} < 1$) [1, 2].

The dependence of the sensor conductivity on the surface potential and temperature has the following form [1–3]

$$G_0(T) = G_{00}(T)\exp\left(-\frac{e\varphi_S(T)}{kT}\right), \tag{2}$$

where

$$G_{00}(T) = \left(\frac{eS_k}{kT}M\right)\frac{e\mu_n E(0)(n_0 + n_V)}{1 + 4\mu_n E(0)/\bar{\upsilon}_n}, \tag{3}$$

M is the constant, whose value depends on the geometric dimensions of the film and tin-dioxide microcrystals, S_k is the contacting area of the neighboring microcrystals, μ_n is the electron mobility in the SnO_2 microcrystals, $E(0)$ is the strength of electric field on the boundary of contacting microcrystals, n_0 is the equilibrium electron concentration in the microcrystals, equal to the concentration of ions of the shallow donor impurity Sb, n_V is the concentration of electrons generated by ionization of oxygen vacancies, and $\bar{\upsilon}_n$ is an average thermal velocity of electrons.

For operation of the sensor in a stationary regime, the dependence of G_0 on T passes through the maximum at a certain temperature $T_M > 473$ K. At $T > T_M$, $G_0(T)$ sharply decreases with increasing temperature due to the increase in $e\varphi_S(T)/(kT)$ and corresponding decrease in $\exp[-e\varphi_S(T)/(kT)]$ [1, 2]. The value of $G_{00}(T)$ only weakly depends on the temperature change. An increase in the energy band bending with increasing T is caused by an increase in the surface density N_i of oxygen ions (O^-) adsorbed on the surface of the SnO_2 microcrystals, since $e\varphi_S(T) \sim N_i^2$ [4, 5].

It follows from Eq. (2) that the energy band bending can be determined by measuring the stationary values of G_0 for two different temperatures of the sensor and the same value of $e\varphi_S$. Adsorption of oxygen ions is an inertial process. For small changes of N_i and $e\varphi_S$, the relaxation time of this process is described by the formula [4]

$$\tau_a = \frac{\exp[E_{D0}/(kT)]}{\nu(1 + \eta_O n_{O_2})}, \tag{4}$$

where E_{D0} is the activation energy of the desorption of oxygen ions, ν is the eigenfrequency of an adsorbed ion, η_O is the coefficient similar to η_H for oxygen, and n_{O_2} is the oxygen concentration in the gas mixture. In accordance with formula (4), τ_a decreases sharply with increasing temperature. This fact can be used to solve the assigned task.

In view of the above, in the heating cycle, the temperature T_2 of the sensor operating in the thermo-cyclic mode is chosen to establish the stationary values of $e\varphi_S(T_2)$ and $G_0(T_2)$ to the end of this cycle. In the cooling cycle, the

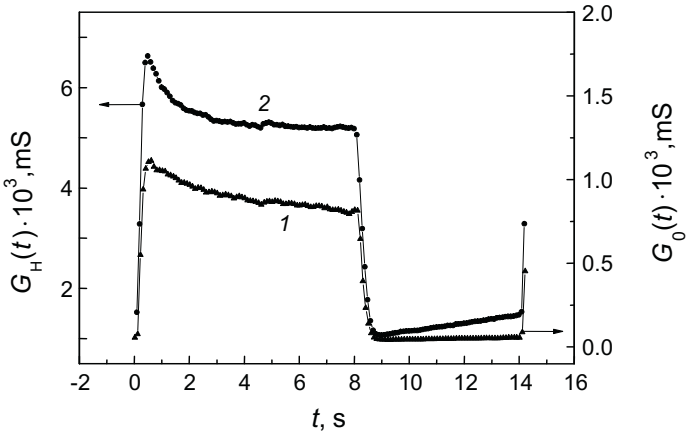

Fig. 1. Time dependences of the conductivity G_0 of the sensor No. 1 in the atmosphere of clean air (*1*) and G_H under exposure to the mixture air + 100 ppm hydrogen (*2*).

temperature T_1 of the sensor should be significantly lower, to keep the value of the energy band bending $e\varphi_S(T_2)$ unchanged for some time after rapid decrease in temperature from T_2 to T_1. To achieve this, the temperature drop of the sensor must be sufficiently quick.

In addition, the sensor temperature in the cooling cycle must satisfy the condition $T_1 \geq 473$ K. At these temperatures, the O^- ions are adsorbed on the SnO_2 surface. At $T_1 < 473$ K, the O_2^--ions are adsorbed [5]. Adsorption of the O_2^--ions is characterized by other values of η_O, E_{D0}, and $e\varphi_S$. And, most importantly, as the temperature of the tin-dioxide film increases, the surface density of the O^--ions is increased and that of the O_2^--ions is reduced [5].

For realization of the thermo-cyclic mode, an automated test stand that allowed to register $G_0(t)$ and $G_H(t)$ at a time interval of $\Delta t = 0.01$s and retune the duration of the heating and cooling cycles in a wide temperature range was used. Taking into account the preliminary measurements, the following parameters were chosen: $T_1 = 473$ K and $T_2 = 673$ K. The durations of the heating and cooling cycles were 8 and 6 s, respectively. The sensor temperature was increased from T_1 up to T_2 over about 0.4 s, while it was decreased from T_2 down to T_1 over about 1 s.

Studies of the conductivity-time profiles (CTP) in the selected thermo-cyclic mode were performed for sensors based on the polycrystalline tin-dioxide films obtained by magnetron sputtering of a tin-antimony alloy target (0.49 at.% of Sb) at direct current. The film thickness was about 100 nm. Dispersed layers of catalysts: palladium and then, platinum (the samples numbers 1 and 2) were deposited on the surface of tin dioxide. In sensors numbers 3 and 4, tin-oxide films modified with gold in the bulk and on the surface were used. Manufacturing technology of sensors is described in detail in [6]. The temperature of sensors was set by the platinum heaters deposited on the back side of the 150 μm thick sapphire substrate. The sample size was 0.7 × 0.7 mm with an area of the sensitive layer 0.3 × 0.3 mm.

In the time dependence of the conductivity $G_0(t)$, after a step-wise rise of temperature from T_1 to T_2 at $0.4 < t <$ 7 s, a decrease of conductivity (Fig. 1, curve *1*) caused by a decrease of the surface density N_g of adsorbed neutral hydroxyl groups (OH-groups) and a following increase of N_i due to the adsorption of O^- ions on the vacated sites are observed [5]. At $t > 6.82$ s, stationary values of $N_i(T_2)$, $e\varphi_S(T_2)$, and $G_0(T_2)$.are established.

During quenching of the sensor from T_2 to T_1 over the time $8 < t < 9$ s, $N_i(T_2)$ and $e\varphi_S(T_2)$ do not have time to change significantly, whereas G_0 is reduced in accordance with Eq. (2). In the time interval $8.92 < t < 9.72$ s, $G_0 = \text{const} = G_0(T_1)$ at the energy band bending $e\varphi_S(T_2)$. At $t > 9.72$ s, $G_0(t)$ weakly increases due to the desorption of O^--ions and increase of N_g. Taking into account the above facts, we obtain from Eq. (2)

$$e\varphi_S(T_2) = \frac{kT_1T_2}{T_2 - T_1} \ln\left[\frac{G_0(T_2)/G_{00}(T_2)}{G_0(T_1)/G_{00}(T_1)}\right]. \quad (5)$$

TABLE 1. Characteristics of Sensors in the Clean Air Atmosphere

No. of sensor	No. of experiment	$G_0(T_2)\cdot 10^4$, mS	$G_0(T_1)\cdot 10^5$, mS	$G_0(T_2)/G_0(T_1)$	$e\varphi_S(T_2)$, eV
1	1	7.85	3.63	21.6	0.46
	2	8.51	3.98	21.4	0.46
	3	8.30	3.82	21.7	0.46
2	1	12.10	8.32	14.5	0.40
	2	13.20	9.4	14.1	0.40
	3	11.90	8.18	14.5	0.40
3	1	66.2	74.2	8.92	0.34
4	1	40.1	57.0	7.03	0.30

At a rapid decrease of the sensor temperature, μ_n, $\bar{\upsilon}_n$, and $n_0 + n_V$ can change their values in Eq. (3) determining $G_{00}(T)$. According to [7], in SnO_2 films, where the channel component of conductivity is dominated, $\mu_n \approx 150$ cm^2/(V s) practically does not depend on T in the temperature range 473–673 K and corresponds to the value of electron mobility in the bulk of microcrystals. In this case, a total electron density $n_0 + n_V$ decreases by about 2 times. The antimony atoms and oxygen vacancies are completely ionized in this temperature range, because their ionization energies are low [8]. Therefore, the decrease in $n_0 + n_V$ with increasing T is due to the decrease in the concentration of oxygen vacancies [2]. Since the process of establishing a steady-state concentration of oxygen vacancies is an inertial one, n_V can be assumed constant at a rapid decrease in temperature.

Assuming $\bar{\upsilon}_n \sim \sqrt{T}$, the dependence G_{00} on T can be characterized by the two extreme cases in accordance with Eq. (3). For $4\mu_n E(0)/\bar{\upsilon}_n << 1$, $G_{00}(T) = B_1/T$ and for $4\mu_n E(0)/\bar{\upsilon}_n >> 1$, $G_{00}(T) = B_2/\sqrt{T}$, where B_1 and B_2 are the constants. Then, for $G_0(T)$, the following expression is valid:

$$G_0(T) = \frac{\text{const}}{T^n}\exp\left[-\frac{e\varphi_S(T)}{kT}\right], \tag{6}$$

where at $n = 1$, the constant = B_1 and at $n = 0.5$, the constant = B_2. Substituting Eq. (6) into Eq. (5), we obtain

$$e\varphi_S(T_2) = \frac{kT_1T_2}{T_2 - T_1}\ln\left[\frac{G_0(T_2)}{G_0(T_1)}\left(\frac{T_2}{T_1}\right)^n\right]. \tag{7}$$

Ambiguity in the choice of the value of n is the source of a possible systematic error in the determination of $e\varphi_S(T_2)$. In this connection, in processing the experimental data, it is advisable to calculate an average value of $e\varphi_S(T_2)$ corresponding to $n = 0.75$. In this case, the maximum possible systematic error in the determination of $e\varphi_S(T_2)$ is: $\Delta[e\varphi_S(T_2)] = \left|e\varphi_{S1}(T_2) - \overline{e\varphi_S(T_2)}\right| = [kT_1T_2/(T_2 - T_1)]\ 0.25\cdot\ln(T_2/T_1) = 0.012$ eV, where $e\varphi_{S1}(T_2)$ corresponds to $n = 1$. To exclude the influence of the humidity on the value of $e\varphi_S(T_2)$ [1, 2], the measurements of $G_0(T_2)$ and $G_0(T_1)$ were performed at the same level of relative humidity RH = 30%.

The data presented in Table 1 show good repeatability of the values $G_0(T_2)/G_0(T_1)$ and $e\varphi_S(T_2)$ in the three series of successive experiments. A random error in determining $e\varphi_S(T_2)$ is 5–10 times less, than the systematic error $\Delta[e\varphi_S(T_2)] = 0.012$ eV. Therefore, considering this error, Table 1 shows the values of $e\varphi_S(T_2)$ up to the second decimal place.

The values of $e\varphi_S$ at $T = 673$ K are practically the same as the values determined using the dependence G_H/G_0 on n_{H_2} for the sensor in an isothermal operation mode [1, 2]. It follows from Eq. (1) that at $\eta_H n_{H_2} >> 1$, the sensor response reaches the maximum possible value $(G_H/G_0)_{max} = \exp[e\varphi_S/(kT)]$. Therefore, we have $e\varphi_S = kT\ln(G_H/G_0)_{max}$.

The results of the repeated measurements (Table 2) performed for the sensors No. 1 and No. 2 after 14 days at the same level of humidity RH = 30% show that $e\varphi_S$ is increased by 0.05–0.06 eV. The upward trend in $e\varphi_S$ with

TABLE 2. Characteristics of Sensors in the Clean Air Atmosphere

No. of sensor	No. of experiment	$G_0(T_2)\cdot 10^4$, mS	$G_0(T_1)\cdot 10^5$, mS	$G_0(T_2)/ G_0(T_1)$	$e\varphi_S(T_2)$, eV
1	1	4.86	1.48	32.8	0.51
	2	4.79	1.46	32.9	0.51
	3	4.77	1.46	32.7	0.51
2	1	8.12	3.76	21.6	0.46
	2	7.76	3.78	20.5	0.45
	3	7. 42	3.43	21.6	0.46

increasing storage or operation time was also observed for several other sensors. Apparently, despite the thermal annealing at 723 K for 24 hours, which is always carried out after the tin-dioxide film deposition, a surface reconstruction can occur during operation of sensors leading to an increase in the surface density of adsorption centers for O^- ions.

2. TIME DEPENDENCE OF THE SENSOR CONDUCTIVITY IN THE THERMO-CYCLIC MODE IN A GAS MIXTURE CONTAINING HYDROGEN

For sensors with the dispersed Pt/Pd layers on the SnO_2 surface, the temperature dependence of G_H/G_0 at n_{H_2} = const passes through a maximum in the vicinity of $T = 673$ K [6]. Therefore, it is advisable to choose 673 K as the working temperature of the sensor in determining n_{H_2}.

In sensors exposed to the air + H_2 mixture, an increase in the conductivity $G_H(t)$ (Fig. 1, curve *2*) is observed in the cooling cycle at $t \geq 9$ s due to the dissociative adsorption of hydrogen on the centers occupied by O^--ions, which leads to an increase in N_g and a decrease in N_i and $e\varphi_S$. Conversely, after the rapid increase of the sensor temperature from T_1 to T_2, neutral hydroxyl groups are intensively desorbed. The O^--ions are adsorbed on the vacant centers, which results in a sharp decrease of $G_H(t)$ with time. At $t \geq 5$ s, a stationary value of $G_H(T_2)$ is established (see Fig. 1, curve *2*).

Using the values $G_H(T_2)$, $G_0(T_2)$, and $e\varphi_S(T_2)$ obtained in the experiment, we can calculate the relation

$$\frac{\ln\left[G_H(T_2)/G_0(T_2)\right]}{e\varphi_S(T_2)/(kT_2)} = \frac{\eta_H n_{H_2}}{1+\eta_H n_{H_2}}\left(2 - \frac{\eta_H n_{H_2}}{1+\eta_H n_{H_2}}\right). \tag{8}$$

It follows from Eq. (8) that

$$\eta_H n_{H_2} = \sqrt{1+\frac{r_1}{1-r_1}} - 1, \tag{9}$$

where

$$r_1 = \frac{\ln\left[G_H(T_2)/G_0(T_2)\right]}{e\varphi_S(T_2)/(kT_2)}. \tag{10}$$

In accordance with Eq. (1), the parameter η_H is calculated by formula [2]

$$\eta_H = \frac{1}{n_{H_2}}\left[\sqrt{1+\frac{\ln(G_H/G_0)}{e\varphi_S/(kT) - \ln(G_H/G_0)}} - 1\right] \tag{11}$$

TABLE 3. Gas Sensitive Characteristics of Sensors

No. of sensor	$G_H(T_2)/G_0(T_2)$	r_1	$\eta_H n_{H_2}$	n_{H_2}, ppm	n'_{H_2}, ppm	Δn_{H_2}, ppm
1	7.43	0.228	0.138	120	100	+20
	64.4	0.47	0.37	330	300	+30
	208	0.61	0.60	530	600	–70
2	6.47	0.235	0.143	120	100	+20
	39.1	0.47	0.37	330	300	+30
	135	0.62	0.62	550	600	–50

using the relations G_H/G_0 obtained for the sensor in isothermal operation mode (T = const). Since the concentration n_{H_2} in the measuring chamber was set using a dosing syringe with a certain error, the value of η_H varied from $1.02\cdot10^{-3}$ to $1.25\cdot10^{-3}$ ppm^{-1} in different experiments [1, 2]. Therefore, an average value of $\eta_H = 1.13\cdot10^{-3}$ ppm^{-1} was used in this paper to calculate n_{H_2}. Maximum possible deviation of η_H from an average value was $\Delta\eta_H \approx \pm0.12\cdot10^{-3}$ ppm^{-1} or $(\Delta\eta_H/\eta_H)\cdot100 \approx 10\%$. The same systematic error is possible in the calculation of n_{H_2}. The random experimental error did not exceed 4%. In calculations of $r_1$by formula (10), the values of $e\varphi_S(T_2)$ given in Table 2 were used.

The results of determination of the hydrogen concentration using the proposed method are shown in Table 3. Approximately the same values of $G_H(T_2)/G_0(T_2)$ and n_{H_2} are obtained for the sensors in isothermal operation mode. Table 3 shows that $(\Delta n_{H_2} / n_{H_2})\cdot100$ does not exceed 20%. Here, $\Delta n_{H_2} = n_{H_2} - n'_{H_2}$, where n'_{H_2} is the concentration of hydrogen set in the measuring chamber by the dosing syringe. Taking into account possible errors in determining and setting the hydrogen concentration, a coincidence of n_{H_2} and n'_{H_2} can be considered as good enough.

Minimum possible value of the response that can be reliably measured, taking into account the experimental errors, is $G_H(T_2)/G_0(T_2) \approx 1.1$, which corresponds to $n_{H_2} = 5$ ppm. The sensor sensitivity is $\beta_1 = \Delta[G_H(T_2)/G_0(T_2)]/\Delta n_{H_2}$ = 0.08 ppm^{-1} at n_{H_2} = 100 ppm. For n_{H_2} equal to 10^3 and $5\cdot10^3$ ppm, β_1 is 1.72 and 0.25 ppm^{-1}, respectively. Calculations of β_1 are performed for the sensor No. 1 using Eq. (1) at Δn_{H_2} = 10 ppm. At high concentrations of hydrogen ($n_{H_2} \geq 10^4$ ppm), the response reaches the maximum possible value $G_H(T_2)/G_0(T_2) = \exp[e\varphi_S(T_2)/kT_2)]$ [1, 2] and $\beta_1 = 0$. At these values of n_{H_2}, the sensor can be used as an indicator of the presence of hydrogen in the gas mixture.

The values of n_{H_2} practically coincident with those shown in Table 3 can be obtained by using the ratio $G_H(T_2)/G_0(T_1)$ as the response. The sensor conductivity in the air + hydrogen mixture is described by the formula given in [1, 2]

$$G_H(T) = G_{00}(T)\exp\left[-\frac{e\varphi_S(T)}{kT(1+\eta_H n_{H_2})^2}\right]. \quad (12)$$

Using Eqs. (2) and (12), we obtain

$$\frac{G_H(T_2)}{G_0(T_1)} = \left(\frac{T_1}{T_2}\right)^n \exp\left\{\frac{e\varphi_S(T_2)}{kT_2}\left[\frac{T_2}{T_1} - \frac{1}{(1+\eta_H n_{H_2})^2}\right]\right\}. \quad (13)$$

Then, we have

$$\eta_H n_{H_2} = \frac{1}{\sqrt{T_2/T_1 - r_2}} - 1, \quad (14)$$

where

TABLE 4. Gas Sensitive Characteristics of Sensors

No. of sensor	$G_H(T_2)/G_0(T_1)$	r_2	$\eta_H n_{H_2}$	n_{H_2}, ppm	n'_{H_2}, ppm	Δn_{H_2}, ppm
1	244	0.65	0.14	120	100	+20
	2100	0.90	0.39	340	300	+40
	6800	1.03	0.60	530	600	–70
2	121.5	0.64	0.13	120	100	+20
	790	0.89	0.37	330	300	+30
	2900	1.04	0.62	550	600	–50

$$r_2 = \ln\left[\frac{G_H(T_2)}{G_0(T_1)}\left(\frac{T_2}{T_1}\right)^n\right] \Big/ \left[\frac{e\varphi_S(T_2)}{kT_2}\right]. \quad (15)$$

The results of the experiment are shown in Table 4. At $T_2/T_1 = 1.42$, the minimum possible value is $r_2 \approx 0.43$, which corresponds to $\eta_H n_{H_2} \approx 0.005$ and $n_{H_2} \approx 4.4$ ppm. Equation (15) shows that at $r_2 \approx 0.43$, the sensor response is $G_H(T_2)/G_0(T_1) = 33.7$. The sensitivity of the sensor No. 1 is 2.5, 52, and 7.69 ppm^{-1} for the hydrogen concentrations of 100, 10^3, and $5\cdot10^3$ ppm, respectively. To calculate β_2, Eq. (13) was used at $\Delta n_{H_2} = 10$ ppm. Thus, β_2 is about 30 times higher, than β_1. At high hydrogen concentrations ($n_{H_2} \geq 10^4$ ppm), the response reaches the maximum possible value $G_H(T_2)/G_0(T_1) = (T_1/T_2)^n \exp[e\varphi_S(T_2)/(kT_1)]$. In this case, $\beta_2 \approx 0$.

At all values of n_{H_2}, the ratio $G_H(T_2)/G_0(T_1)$ is 33 and 20 times higher than $G_H(T_2)/G_0(T_2)$ for the sensors No. 1 and No. 2, respectively (see Tables 3 and 4). Approximately the same difference is observed for the ratios of the sensor sensitivities. Thus, for determining the concentration of hydrogen in a gas mixture, it is advisable to use the ratio $G_H(T_2)/G_0(T_1)$. In this case, $G_H(T_2)$ and $G_0(T_1)$ should be measured at about the same time, which can be carried out only when the sensor operates in the thermo-cyclic mode.

CONCLUSIONS

Based on a detailed analysis of the time dependence of the sensor conductivity $G_0(t)$ in the atmosphere of clean air when operation of the sensor in the thermo-cyclic mode, a method for determining the energy band bending $e\varphi_S$ at the interface of the contacting SnO_2 microcrystals in the polycrystalline tin-dioxide film is proposed. The values of $e\varphi_S$ obtained at $T = 673$ K are close to those determined for the sensor operating in a isothermal operation mode. It is established that during storage or operation of sensors, $e\varphi_S$ is gradually increased indicating that the density of adsorption sites for O^- ions on the surface of the SnO_2 microcrystals is increased.

At a correct choice of parameters of the thermo-cyclic mode (the time periods and the temperatures in the heating and cooling cycles) with taking into account the adsorption-desorption processes on the surface of the SnO_2 microcrystals, the proposed method can be used to determine $e\varphi_S$ also at $T \neq 673$ K.

Based on the analysis of the time dependence of the conductivity $G_H(t)$ of sensors operating in a gas mixture containing hydrogen (air + H_2), two methods for determining n_{H_2}. are proposed. In the first method, as in a isothermal operation mode, a ratio of the stationary values of G_H to G_0 at $T = 673$ K is used as the sensor response to the impact of hydrogen. In the second method, the relation $G_H(673\text{ K})/G_0(473\text{ K})$ is chosen as the sensor response. It follows from the results of the experiment that for the values of n_{H_2} in the interval 100–600 ppm, the responses of the first and the second examined sensors determined using the second method are 33 and 20 times, respectively, higher than those determined using the first method.

The experimental results and theoretical estimates presented in this paper show that the sensors based on thin polycrystalline tin-dioxide films in the thermo-cyclic operation mode are characterized by high values of sensitivity and response at low hydrogen concentrations. At $n_{H_2} \approx 5$ ppm, $G_H(673\text{ K})/G_0(473\text{ K}) \approx 34$ and at $n_{H_2} \approx 600$ ppm, the

responses are 6800 and 2900 for the two examined sensors. The maximum possible response (at $\eta_H n_{H_2} >> 1$) is of about $2 \cdot 10^5$ for the first sensor and $6 \cdot 10^4$ for the second one. The calculated sensitivities $\Delta[G_H(673\ K)/G_0(473\ K)]/\Delta n_{H_2}$ of the first sensor are 2.5, 52, and 7.69 ppm^{-1} at n_{H_2} equal to 100, 10^3, and $5 \cdot 10^3$ ppm, respectively.

The investigated sensors have high speed response. The change of the hydrogen concentration in the gas mixture may be detected after 15–20 s. Thus, sensors based on thin tin-dioxide films can be used to produce highly sensitive and high-speed detectors of low concentrations of hydrogen.

This work was supported in part by the grant of Federal Target Program (State Contract No. 14.740.11.1018, 23 May 2011).

REFERENCES

1. V. I. Gaman, Russ. Phys. J., **51**, No. 4, 425–432 (2008).
2. V. I. Gaman, Physics of Semiconductor Gas Sensors, Izd. Nauchn. Tekh. Liter., Tomsk (2012).
3. V. I. Gaman, Russ. Phys. J., **54**, No. 12, 1364–1371 (2012).
4. V. I. Gaman, Russ. Phys. J., **54**, No. 10, 1137–1144 (2012).
5. G. Korotcenkov, V. Brinsari, V. Golovanov, *et al*., Sensors and Actuators. B, **98**, 41–45 (2004).
6. E. Yu. Sevast'yanov, N. K. Maksimova, V. A. Novikov, *et al*., Fiz. Tekh. Poluprovodn., **46**, No. 6, 820–828 (2012).
7. S. I. Rembeza, T. V. Svistova, O. I. Borsyakova, *et al*., Semiconductors, **35**, No. 7, 762–765 (2001).
8. S. Samson and C. G. Fonstad, J. Appl. Phys., **44**, No. 10, 4618–4621 (1973).